



This is a repository copy of *A new two-dimensional model of rolling-sliding contact creep curves for a range of lubrication types.*

White Rose Research Online URL for this paper:  
<http://eprints.whiterose.ac.uk/76102/>

Version: Accepted Version

---

**Article:**

Fletcher, D.I. (2013) A new two-dimensional model of rolling-sliding contact creep curves for a range of lubrication types. *Proceedings of the Institution of Mechanical Engineers, Part J: Journal of Engineering Tribology*, 227 (6). 529 - 537. ISSN 1350-6501

<https://doi.org/10.1177/1350650112465694>

---

**Reuse**

Unless indicated otherwise, fulltext items are protected by copyright with all rights reserved. The copyright exception in section 29 of the Copyright, Designs and Patents Act 1988 allows the making of a single copy solely for the purpose of non-commercial research or private study within the limits of fair dealing. The publisher or other rights-holder may allow further reproduction and re-use of this version - refer to the White Rose Research Online record for this item. Where records identify the publisher as the copyright holder, users can verify any specific terms of use on the publisher's website.

**Takedown**

If you consider content in White Rose Research Online to be in breach of UK law, please notify us by emailing [eprints@whiterose.ac.uk](mailto:eprints@whiterose.ac.uk) including the URL of the record and the reason for the withdrawal request.



[eprints@whiterose.ac.uk](mailto:eprints@whiterose.ac.uk)  
<https://eprints.whiterose.ac.uk/>

# **A new two-dimensional model of rolling-sliding contact creep curves for a range of lubrication types**

DI Fletcher\*

Department of Mechanical Engineering, University of Sheffield, Mappin Street, Sheffield, UK S1 3JD

\* Corresponding author, Tel +44 114 2227760, Fax +44 114 2227890, Email [D.I.Fletcher@sheffield.ac.uk](mailto:D.I.Fletcher@sheffield.ac.uk)

## **ABSTRACT**

Experimentally determined creep curves for rolling-sliding contact in lubricated conditions are found to deviate greatly from the standard theory for two body contact. This paper presents a new model to represent coefficient of adhesion (also known as traction coefficient) and creep based on experimental data gathered for a range of railway rail-wheel contact conditions. The model developed is based on a 2D elastic foundation representation of a twin disc contact. This is used to quantify the creep curves in a similar manner to existing 3D models of real rail-wheel contacts undergoing partial slip for a range of lubrication conditions.

The work focuses on very low levels of creep, ranging from zero to 1%, and lubricants experienced by a rail-wheel contact in service (dry, wet, flange lubricant). Lubricants used during the simulation of low adhesion conditions for driver training (soap and water, lignin and water) are also represented. The motivation for the research is inclusion of creep-traction characteristics in an on-board system being developed for prediction of low adhesion conditions at the rail-wheel interface based upon monitoring running conditions prior to brake application.

Keywords: rail-wheel, adhesion, model, 2D, creep, lubrication, railway

## **Nomenclature**

$a$  – contact half width

$c$  – half width of the region of adhesion

$E^*$  – combined elastic modulus

$E$  – Young's modulus

$h$  – depth of elastic foundation

$k_a$  – shear traction reduction factor for area of adhesion

$k_s$  – shear traction reduction factor for area of sliding

$K_p$  – elastic modulus of foundation, normal direction  
 $K_q$  – elastic modulus of foundation, tangential direction  
 $P$  – normal contact load  
 $p$  – contact pressure  
 $Q$  – total shear force on the contact  
 $Q_S$  – shear force in slip area of contact  
 $Q_A$  – shear force in adhesion ('stick') area of contact  
 $q_A$  – shear traction in a region of adhesion ('stick')  
 $q_S$  – shear traction in a region of slip  
 $R$  – Reduced radius of curvature, for disc or rail-wheel system  
 $V$  – rolling speed  
 $V_{1,2}$  – surface speed of bodies 1 or 2  
 $x$  – longitudinal axis, in the direction of sliding  
 $\mu$  – friction coefficient  
 $\nu$  – Poisson's ratio  
 $\xi$  – creep ratio in the rolling direction

## **1 Introduction**

Rail-wheel contacts operate in a combination of rolling and sliding motions, with small amounts of creep between the surfaces produced during braking, acceleration, steering, and through the non-conformal geometry of the rail-wheel contact. In cases of rail contamination, including autumn leaf debris from surrounding trees, rail-wheel adhesion can fall to a level insufficient for normal acceleration or braking to be maintained. In these cases damage to rail and wheels can result from wheel slip or wheel spin, and there can be safety consequences such as signals passed at danger (SPADS) [1].

Coefficient of adhesion (CoA, also often referred to as coefficient of traction) is defined as the ratio of tangential adhesion force ( $Q$ ) to normal force ( $P$ ) on the rail-wheel contact. Guidance notes on low adhesion measurement available from the Railway Safety and Standards Board (RSSB) [2] state that to sustain normal braking a CoA of 0.14 or above is required. Beyond warnings at sites where low adhesion frequently occurs, and seasonal warnings linked to weather and leaf fall, there is

currently little or no advance warning available to the driver that a train has entered a site of low adhesion until brake application produces poor or insufficient deceleration. To improve this situation research is underway to develop a low adhesion detection system [3] capable of predicting low adhesion prior to brake application. A key component of this is the relationship between CoA and creep at the rail-wheel interface, which is usually represented by a curve such as Figure 1 (shown in non-dimensional form). Critical parameters defining such curves are the creep coefficient at low slip (the gradient of the adhesion coefficient versus creep curve) and the saturation level of adhesion coefficient at full slip (i.e. the friction coefficient).

Figure 1 shows theoretical creep curves but these are found to be unrealistic in many cases. Fletcher and Lewis [4] investigated the link between creep coefficient and friction coefficient by generating a series of creep curves under closely controlled conditions for a range of rail-wheel contact contamination conditions. These data focused on very low levels of creep (0 to 1%) and showed that for contacts lubricated with flange lubricants, greases or lignin (intended to represent leaf debris) there was considerable deviation of the creep curve from the form predicted by conventional rolling-sliding contact theory. To make use of the data from these experiments for low adhesion detection [3] a model was needed for two-dimensional (line) contact with partial slip, but it was found that existing models for contaminated contacts focused primarily on three-dimensional contacts. This paper describes a new model that can successfully represent these data while maintaining a link to the physical stick and slip processes within the contact. It is found that just a single additional parameter beyond those in conventional contact models is needed to represent real creep-force behaviour.

### **1.1 Partial slip contact models**

When a rail and wheel, or the rail and wheel discs in a twin disc test, are brought together under a normal load their surfaces deform in both normal and tangential directions. Within the contact, and depending on the friction coefficient at their interface, the surfaces may move together with no relative motion, or may move by different displacements to one another. This divides the contact into regions of ‘stick’ and ‘slip’ respectively, with stick usually happening at the centre of the contact, and slip happening towards the edges. If the contact is transmitting a shear traction in a

rolling-sliding configuration it is found that the stick region is located at the leading edge of the contact, and the slip happens at the trailing edge [5] as shown in Figure 2. The division of the contact into stick and slip regions in this ‘partial slip’ condition depends on the level of creep relative to the ‘full slip’ case for which transmitted traction equals the product of normal load and friction coefficient. For dry or boundary lubrication cases (including water lubrication) the model by Carter [6] and the elastic foundation model described by Johnson [5] are able to produce very good two dimensional representations of the experimentally determined creep behaviour in the transition from pure rolling, through partial slip to the point of full sliding, and similar models are available for three-dimensional contacts under these conditions [5,7].

For better lubricated or contaminated contacts, the correlation between the Carter or elastic foundation models and the experimental data is poor [3]. Factors of importance for modelling adhesion at rail-wheel contacts in these conditions are summarised by Polach [8] in development of his three-dimensional contact model. These include creep dependence of friction coefficient producing different friction levels in the ‘stick’ and ‘slip’ areas of contact, and consideration of contact shear stiffness reduction caused by an interfacial layer partially separating the rail and wheel. However, the Polach model is not applicable to two-dimensional contact as it relies a contact shear stiffness coefficient derived from Kalker’s linear theory [9] which is inherently three dimensional. Existing two-dimensional models by Carter [6] or the elastic foundation model by Johnson [5] assume a constant underlying friction coefficient and do not consider the factors shown by Polach to be important in real lubricated contacts. Following a summary of experimentally determined creep curve data for a range of conditions, details are given in Section 3 of an addition to the two-dimensional elastic foundation model able to overcome these limitations.

## **2 Summary of experimental data**

This section presents a short summary of the creep curve data generated for a range of common rail-wheel contact conditions using an updated version of the SUROS rolling sliding test machine [10]. Full details of the tests and the updates made to the machine to generate this data are reported elsewhere [3]. This machine is able to maintain

closed loop control of creep between rail and wheel disc samples of 47mm diameter, each cut out of parent rail and wheel components to ensure the correct materials are used. The machine was used to perform a programmed variation of creep starting from pure rolling and increasing to 1% over 60 minutes thereby maintaining a quasi-static creep condition at any moment, and generating an entire creep curve within a single test. In all cases the test was for a driving wheel, i.e. negative creep using the conventional definition shown in Equation (1), but all values are presented here as positive numbers to give conventional creep curve diagrams. The tests used a normal grade 220 rail of hardness  $237\text{HV}_{(100\text{kg})}$  and an R8 wheel of hardness  $257\text{HV}_{(100\text{kg})}$  [11].

$$\text{Creep}(\%) = 200 \frac{R_{\text{rail}}S_{\text{rail}} - R_{\text{wheel}}S_{\text{wheel}}}{R_{\text{rail}}S_{\text{rail}} + R_{\text{wheel}}S_{\text{wheel}}} \quad (1)$$

Table 1 summarises the test conditions and codes, these codes having been kept identical to the source data [3] although not all the original tests are considered here. The majority of tests were conducted at 1000MPa maximum Hertzian contact pressure, with tests at 800MPa and 1300MPa conducted on a single solid flange lubricant product. Figure 3 presents the creep curve data in a non-dimensional form for all the lubricant types tested at 1000MPa, with creep normalised through multiplying by radius  $R$  and divided by the contact patch half-width  $a$ , and the friction coefficient  $\mu$ . For contact pressures of 800, 1000 and 1300MPa the contact patch half-widths were calculated as 0.163, 0.204 and 0.265mm respectively using a two dimensional line contact Hertzian model [12]. The friction coefficient for each lubricant (as distinct from the adhesion coefficient) was determined from the ‘saturation’ level of the creep curve at which full slip was achieved (Table 1). The adhesion coefficient (tangential force  $Q$  divided by normal force  $P$ ) was normalised by the friction coefficient  $\mu$  to give the vertical axis values.

The ‘theoretical’ curve in Figure 3 was generated using the elastic foundation model [5] in a similar manner to Figure 1. It can be seen that this is able to represent the behaviour of the dry and water lubricated cases, but not the better lubricated conditions.

### 3 A new 2D model to represent creep force

The data generated in the SUROS tests clearly does not all lie on the theoretical creep curve (Figure 3). Here a model for a modified creep curve is developed capable of achieving a very close fit to the experimental data for all the conditions tested.

#### 3.1 Two dimensional elastic foundation contact model

Johnson [5] sets out solutions for an elastic foundation or Winkler model of contact, and explains the choice of stiffness per unit depth of foundation to produce results which closely approximate a Hertzian contact solution. An exact match cannot be achieved since the body considered in an elastic foundation model must be represented by a certain finite foundation depth. However, the approach is used here to achieve features similar to those of Polach's model [8] possibly assisting the later translation of 2D experimental data to 3D application.

For a line contact the normal pressure variation with position through the contact is given by Equation (2), with the elastic modulus of the foundation related to the Young's modulus by Equation (3).

$$p(x) = \frac{K_p}{2Rh} (a^2 - x^2) \quad (2)$$

$$\frac{K_p}{h} = \frac{1.18E^*}{a} \quad (3)$$

Here the combined elastic modulus for the two bodies in contact is defined by Equation (4), although the elastic foundation model is restricted to considering bodies of equal elastic properties.

$$\frac{1}{E^*} = \frac{1 - \nu_{wheel}^2}{E_{wheel}} + \frac{1 - \nu_{rail}^2}{E_{rail}} \quad (4)$$

In areas of the contact experiencing full slip the shear traction is defined by Equation (5) in which  $\mu$  is the friction coefficient. The equation includes a

'reduction factor'  $k_s$  which takes a positive value of 1 or below depending on the behaviour under sliding contact relative to prediction of shear load using the static friction coefficient. This dynamic friction reduction factor has similarity to the reduction factor introduced by Polach [8], however, the formulation of the current model differs from that of Polach, and values of the reduction factors cannot be transferred between the models. Values of this factor must be found by fitting to experimental data.

$$q_s(x) = \mu p(x) = \frac{k_s K_p \mu}{2Rh} (a^2 - x^2) \quad (5)$$

If a sticking region exists within the contact this will start at the leading edge, and Johnson shows that the shear traction increases linearly from zero at the leading according to Equation (6), Figure 2, with creep ratio defined by Equation (7). Johnson states that to coincide with the half-space solution, the tangential modulus of the foundation  $K_q$  should be 2/3 the value of the normal modulus  $K_p$ . Similar to the sliding region of the contact a 'reduction factor'  $k_a$  is introduced for the area of adhesion. Again, this is not the same reduction factor defined by Polach [8] so numbers are not interchangeable between the models, but the concept is similar.

$$q_A(x) = -\frac{k_a K_q \xi}{h} (a + x) \quad (6)$$

$$\xi = \frac{V_1 - V_2}{V} \quad (7)$$

For a case in which slip occurs Figure 2 illustrates the resulting distributions of normal and tangential tractions. Defining the region of adhesion to be of width  $2c$  the position of the transition between stick and slip can be found. Remembering that (i) the ratio of tangential to normal modulus for the elastic foundation must be 2/3, and that (ii) under high creep the dimension  $c$  will reduce to zero but cannot become negative, gives Equation (8).

$$c = \max\left(a - \frac{k_a K_q \xi R}{k_s K_p \mu}, 0\right) = \max\left(a - \frac{2k_a \xi R}{3k_s \mu}, 0\right) \quad (8)$$

Johnson [5] presents a solution to enable total friction force to be found for the combined stick and slip regions in the form of an overall adhesion coefficient. It is useful here to derive that relationship in a different form, with separate components for adhesion and slip areas. In the adhesion region ('stick', width  $2c$ ) the shear force ( $Q_A$ ), normalised by total applied load ( $P$ ) is given by Equation (9), derived from the gradient of the tangential stress curve defined by Equation (7) and the area of the triangular region beneath it.

$$\frac{Q_A}{P} = \frac{2c^2}{P} \frac{d}{dx} \left( \frac{k_a K_q \xi}{h} (a+x) \right) = \frac{2k_a c^2 \xi R}{a^3} \quad (9)$$

The normal force  $P$  is given by equation (10).

$$P = \frac{2K_p a^3}{3hR} \quad (10)$$

In the slipping region, the shear force transmitted is given by Equation (11) which was generated by integrating Equation (5) between the limits  $2c-a$  to  $a$ .

$$\frac{Q_S}{P} = \frac{1}{P} \int_{-a}^{a-2c} \frac{k_s K_p \mu}{2Rh} (a^2 - x^2) dx = \frac{3}{2} \frac{\mu k_s (a-c)}{a} - \frac{1}{4} \frac{\mu k_s (a^3 - (2c-a)^3)}{a^3} \quad (11)$$

Taking the stick and slip regions together, Equation (12) gives the total creep force for a partially slipping line contact based on the elastic foundation model, including reduction factors allowing representation of real contact behaviour.

$$\frac{Q}{P} = \frac{Q_A}{P} + \frac{Q_S}{P} = \underbrace{\frac{2k_a c^2 \xi R}{a^3}}_{\text{Adhesion region}} + \underbrace{\frac{3}{2} \frac{\mu k_s (a-c)}{a} - \frac{1}{4} \frac{\mu k_s (a^3 - (2c-a)^3)}{a^3}}_{\text{Slip region}} \quad (12)$$

## 4 Application of two dimensional model to experimental data

The model described in Section 3.1 was applied for each set of experimental data and the reduction factors used to achieve the best fit between the model and experimental predictions. As an initial stage, and since the data are primarily for very low creep conditions in which the adhesion region of the contact will be important, it was decided to vary just parameter  $k_a$  related to the adhesion region, and to leave parameter  $k_s$  equal to 1. Values of friction coefficient  $\mu$  had been previously defined from the saturation level of adhesion coefficient at full slip [3] and are summarised in Table 1. The data fitting was carried out using the 'fit' function within Gnuplot [13] which implements a nonlinear least-squares Marquardt-Levenberg algorithm. It was found that fitting using just parameter  $k_a$  was so successful that further fitting by variation of  $k_s$ , which is most relevant to contacts operating at creep beyond full slip, was not pursued. The data used here do not enter that region, however, inclusion in the model of the  $k_s$  parameter does offer the opportunity to model for two dimensional contacts the decline in adhesion coefficient at high creep that was represented for three-dimensional contacts by Polach [8], and this is the subject of further research.

Table 2 shows the parameter values produced by fitting the new 2D model to each of the experimental datasets. Figure 4 shows the results for cases of oil, solid lubricated, and dry contacts. In each plot the original model (i.e.  $k_a=1$  and  $k_s=1$ ) is shown together with the experimental data and model output for the values of  $k_a$  shown in Table 2. It can be seen from the figures that the new 2D model is able to produce much better agreement with the experimental data. The refinement is minor in the case of dry contact, for which there is no third body present in the contact, and friction behaviour is closely approximated by the standard model (Figure 3). In the case of well lubricated contacts the original model produced a poor representation of the creep curve, whereas the new model is much better able to capture the slope at low creep values and the gradual transition to full slip. Curves for other lubricants showed similarly very good agreement between the new model and the experimental data.

Figure 5 shows the results of applying the model to creep curves at a range of contact pressures, using the friction coefficient values from Table 1, the  $k_a$  values in Table 2 and taking account of the change in contact patch half-width using the values for  $a$  given in Section 2. The dotted lines in the figure indicate the predictions of the unmodified elastic foundation model for these conditions, showing very poor agreement in the partial slip region at all the contact pressures. Using the new model the curves much better represent the experimental data, although they slightly over-predict the adhesion coefficient in the creep range 0.4-0.6% for contact pressures of 1000 and 1300MPa.

#### **4.1 Physical meaning**

In addition to better representing the experimental data, the new model retains clear contributions to contact shear force from the stick and slip areas of the contact, which allows some insight into the physical meaning of the reduction factors. Figure 6 shows a comparison of the original elastic foundation and new 2D models, indicating how the shear force in the adhesion (stick) and slip areas of contact contributes to the total shear force over a range of low creep values. The figure is based on the oil lubricated test O1 for which the original model was a very poor representation of the data, and the new model with  $k_a=0.193$  much better represents the data. It can be seen that inclusion of the parameter  $k_a$  has the effect of 'stretching' the partial slip area of the creep curve over a much larger range of creep ratio, that is, the physical meaning of the parameter is a delay in the creep at which full slip is achieved. This delay is particularly relevant to well lubricated cases, for which the original model least well represented the experimental data.

## **5 Conclusions**

A two-dimensional model has been developed to represent the real traction-creep behaviour of well lubricated rolling-sliding contacts. The model is able to accurately represent creep curve data gathered from experiments on a twin-disc testing machine under lubrication conditions characteristic of the railway rail-wheel contact. The data for which the model has been demonstrated focus on very low levels of creep, ranging from zero to 1%, for lubrication conditions experienced by a rail-wheel contact in

service (dry, wet, flange lubricant). Those used during the simulation of low adhesion conditions for driver training (soap and water, lignin and water) were also investigated.

The model is based on an elastic foundation representation of the contact, and is able to represent real adhesion behaviour for a two-dimensional contact in the same way that an earlier model by Polach [8] achieves this for three-dimensional contacts. This includes the effect of creep dependent friction coefficient (for example due to temperature differences with slip) and contact shear stiffness reduction caused by an interfacial layer between the rail and wheel steel surfaces. The current model is independent of the coefficients derived from Kalker's linear theory on which the Polach model is based, and which prevent its direct application to two-dimensional contacts.

The motivation for the research was inclusion of adhesion-creep characteristics in an on-board system being developed for prediction of low adhesion conditions at the rail-wheel interface, based upon monitoring running conditions prior to brake application. The model developed provides a simple way to represent real adhesion-creep behaviour, and to link differences in creep coefficient (initial slope of the adhesion coefficient-creep curve) to friction coefficient (saturation level of adhesion coefficient at full slip). Use in a predictive capacity to map contact forces measured at low levels of slip to the maximum available adhesion will support automated detection and warning of low adhesion before braking is attempted.

## **6 Acknowledgements**

The author is grateful to the Railway Safety and Standards Board for their sponsorship of this research, and for the collaboration with Professor Roger Goodall and Dr Chris Ward at Loughborough University that has made the research possible.

## 7 References

1. Poole, W, An Overview of Low Adhesion Factors for ERTMS, Project T080 final report, July 2003, Rail Safety and Standards Board, Block 2, Angel Square, 1 Torrens Street, London EC1V 1NY
2. GM/GN2642 Guidance on Wheel/ Rail Low Adhesion Measurement, Issue One: February 2008, Rail Safety and Standards Board, Block 2, Angel Square, 1 Torrens Street, London EC1V 1NY
3. Onboard detection of low adhesion, Railway Safety and Standards Board project T959, Research and Development E-Newsletter, Issue 69, January 2011, [www.rssb.co.uk](http://www.rssb.co.uk).
4. Fletcher, DI, Lewis, S, Creep curve measurement using a continuously variable creep twin disc machine, submitted to *Wear*, 2012.
5. KL Johnson, *Contact Mechanics*, Cambridge University Press, 1987, Cambridge, UK
6. Carter, FW, On the Action of a Locomotive Driving Wheel, *Proceedings of the Royal Society of London. Series A*, 112, 760 (1926),151-157
7. Haines, DJ, Ollerton, E, Contact stress distribution on elliptical contact surfaces subject to radial and tangential forces, *Proceedings of the Institution of Mechanical Engineers*, 177, 95 (1963) 261-265
8. O. Polach, Creep forces in simulations of traction vehicles running on adhesion limit, *Wear* 258 (2005) 992–1000
9. J.J. Kalker, On the rolling contact of two elastic bodies in the presence of dry friction, Thesis, Delft, 1967.
10. Fletcher D. I. and Beynon, J. H. Development of a machine for closely controlled rolling contact fatigue and wear testing. *J. Test. Eval.*, 2000, 28(4), 267–275.
11. Carroll, RI, Beynon, JH, Rolling contact fatigue of white etching layer: Part 1: Crack morphology, *Wear*, Volume 262, Issues 9-10, 2007, 1253-1266
12. Engineering Science Data Unit Item 78035, Contact phenomena I: stresses, deflections and contact dimensions for normally-loaded unlubricated elastic components, 1995, ESDU International, London.
13. Williams, T, Kelley, C, Gnuplot 4.4, An Interactive Plotting Program, manual available from [www.gnuplot.info](http://www.gnuplot.info).

## Tables

**Table 1.** Lubrication conditions, test codes, friction coefficients (saturation adhesion coefficient) and creep coefficients (initial force-creep gradients) for each test

Lubricant type	Contact pressure, MPa	Test code	Friction coefficient, $\mu$	Creep coefficient
Water	1000	W1	0.24	0.7
Solid lubricant	1000	SL1	0.12	0.45
Solid lubricant	800	SL2	0.16	0.4
Solid lubricant	1300	SL3	0.103	0.4
Soap and water	1000	SW1	0.055	0.2
Oil	1000	O1	0.055	0.24
Track grease TG	1000	TG1	0.09	0.26
Track grease CG	1000	CG1	0.025	0.08
Lignin and water	1000	L1	0.08	0.27
Dry	1000	D3	0.58	0.75

**Table 2.** Parameter values used in new 2D model to achieve fits to the experimental data. The value of  $k_s$  was taken to be 1 in all cases.

Test	$k_a$
W1	0.805
SL1	0.462
SL2	0.306
SL3	0.464
SW1	0.239
O1	0.193
TG1	0.233
CG1	0.0495
L1	0.168
D3	0.808

## Figure Captions

- Figure 1.** Comparison of creep curves from the Carter (Hertzian) and elastic foundation models
- Figure 2.** Distribution of normal pressure and tangential traction across a partially slipping contact.
- Figure 3.** Creep curves for all the lubrication conditions examined, normalised axes. All at 1000MPa maximum Hertzian contact pressure.
- Figure 4.** Creep curves, with experimental data alongside curves from the original and new 2D contact models. (a) Oil lubricated contact, test O1. (b) Data for solid lubricant from test SL1. (c) Dry test, D3.
- Figure 5.** Creep curves for tests on solid flange lubricant at a range of contact pressures. Experimental data (points), predictions of original model (dotted lines) and new model (solid lines).
- Figure 6.** Creep curves for the original and new 2D model, plotted for oil lubricated test O1. For each model the total creep force curve is shown alongside the contributions from the stick (adhesion) and slip areas of the contact. Parameters for the model are taken from Table 1 and Table 2.

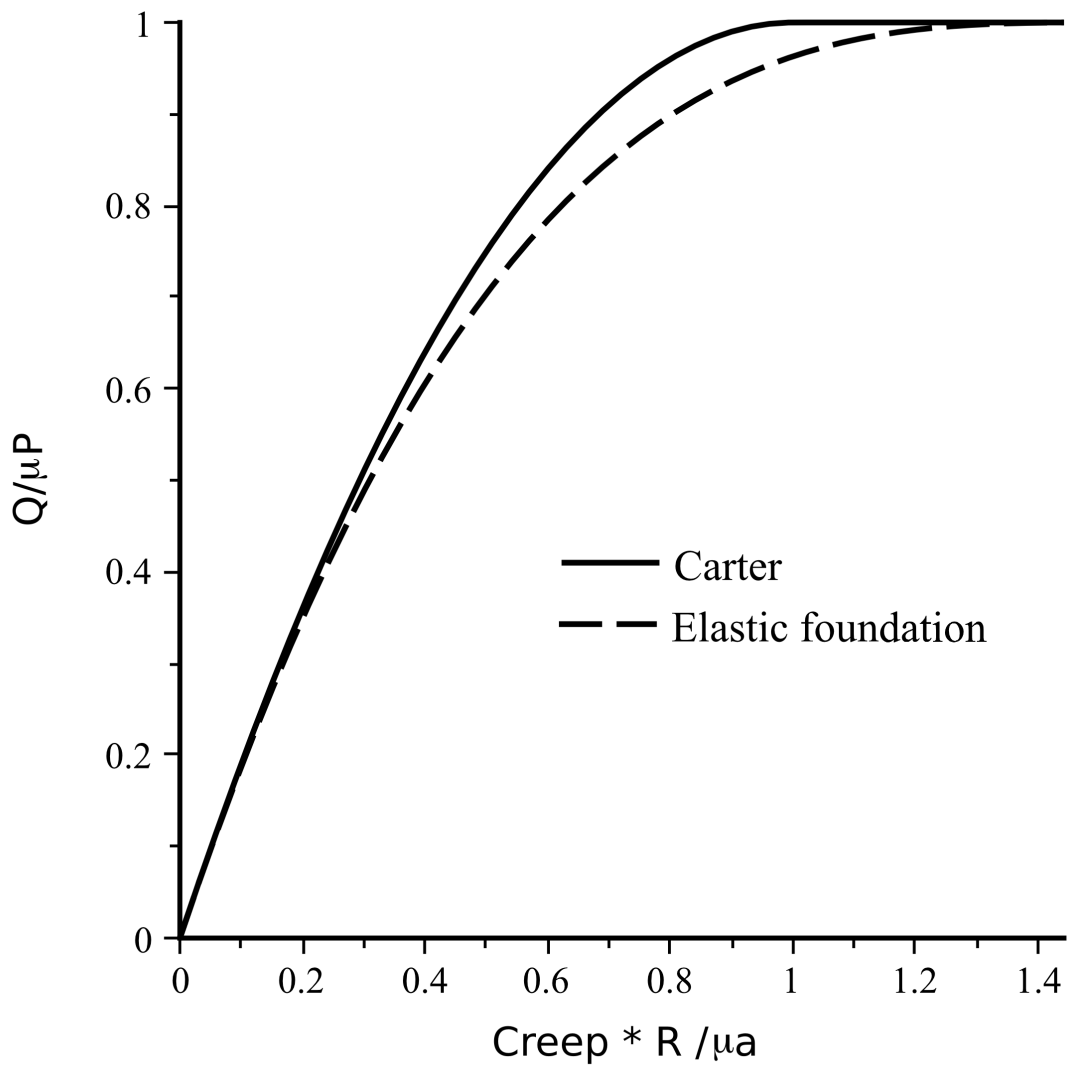


Figure 1

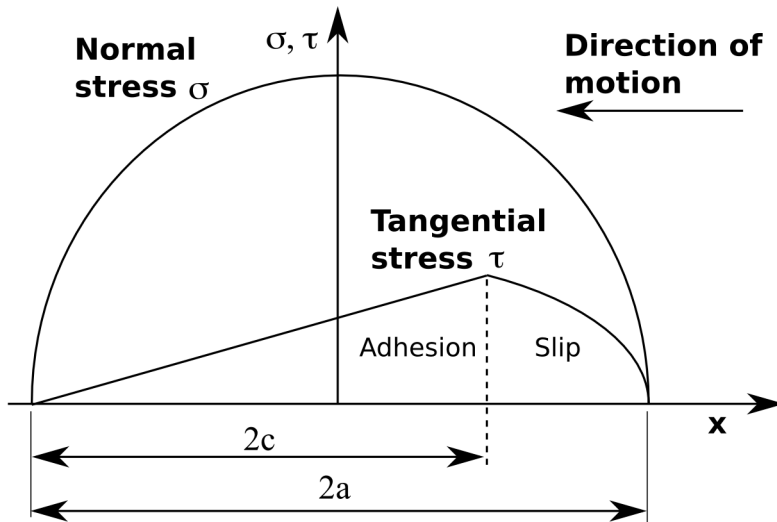


Figure 2

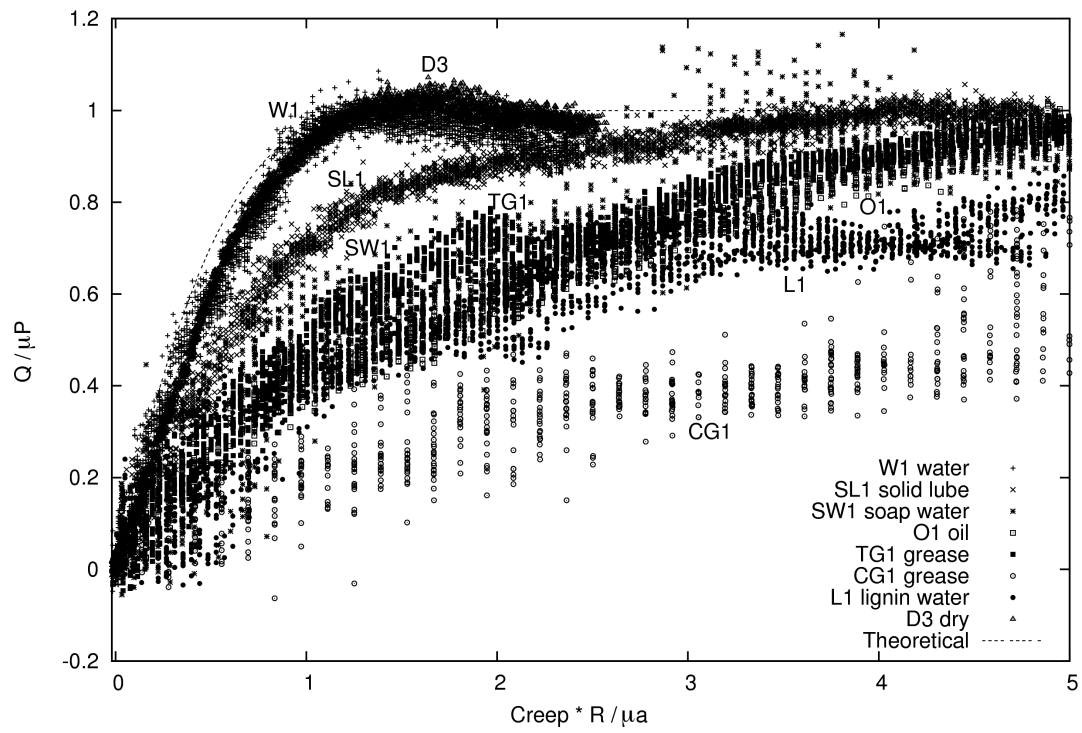


Figure 3

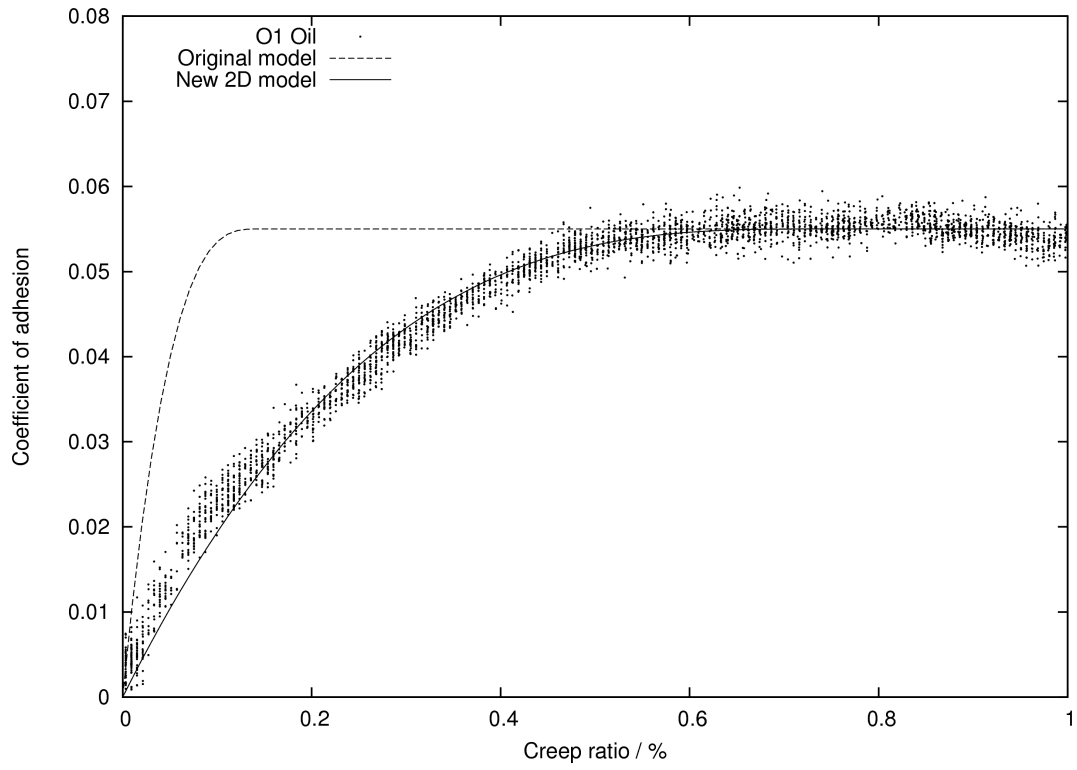


Figure 4a

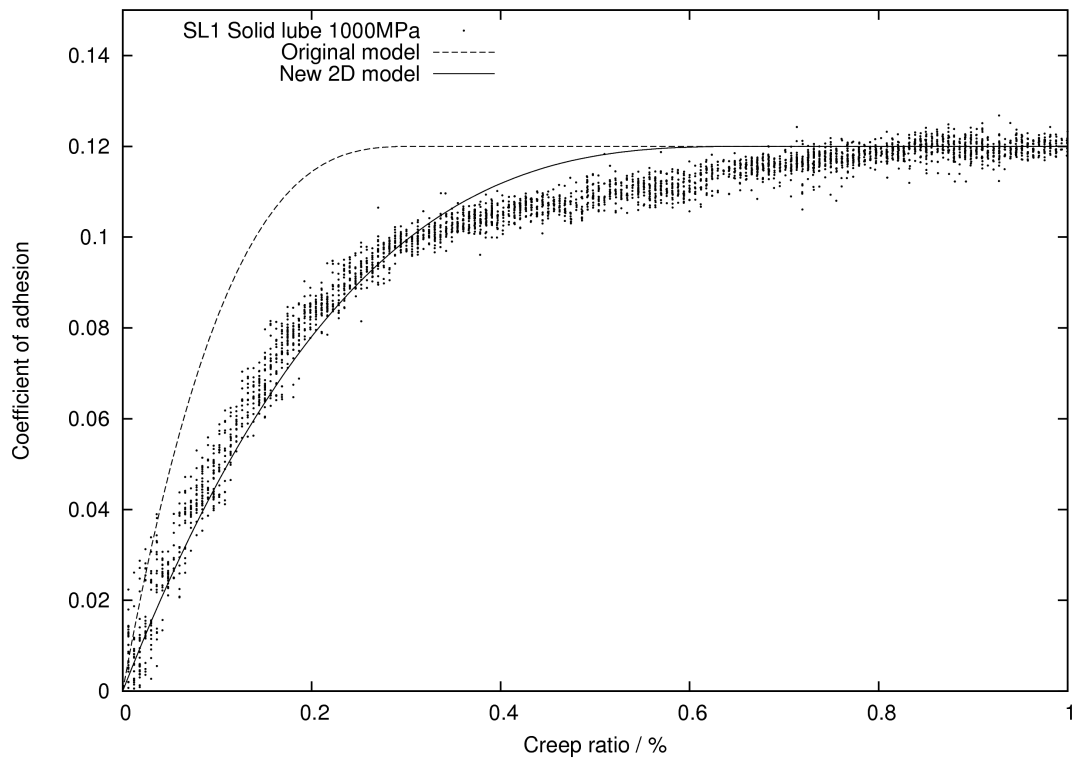


Figure 4b

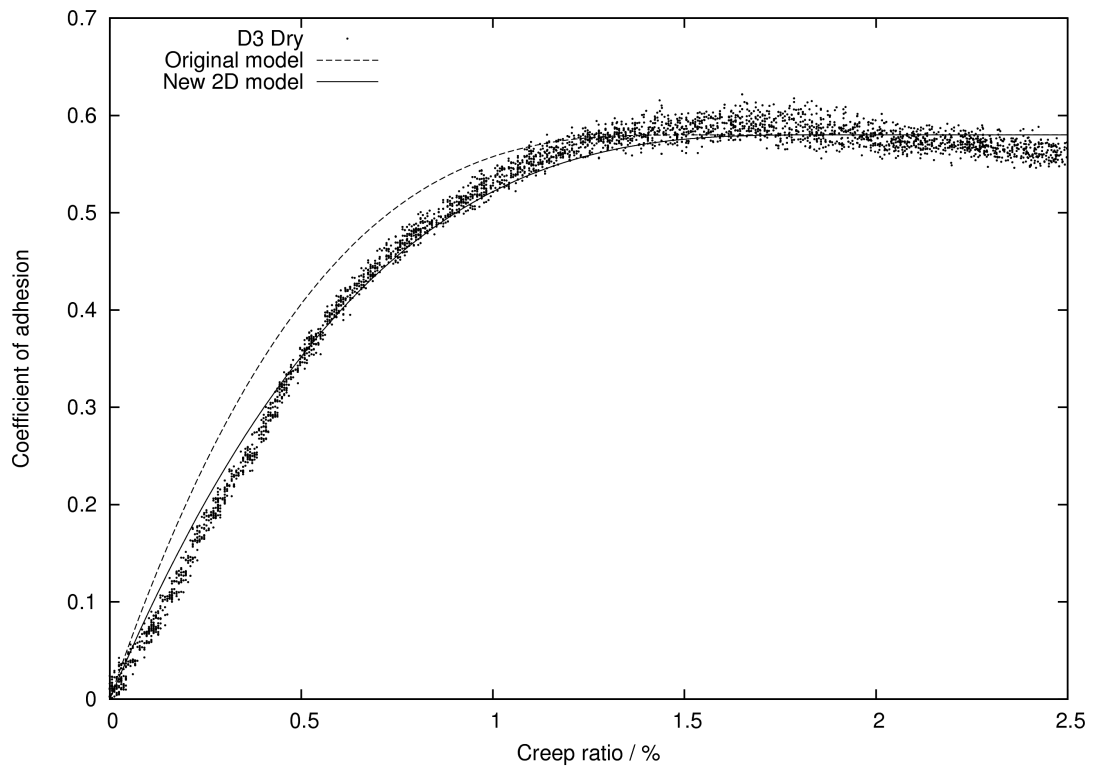


Figure 4c

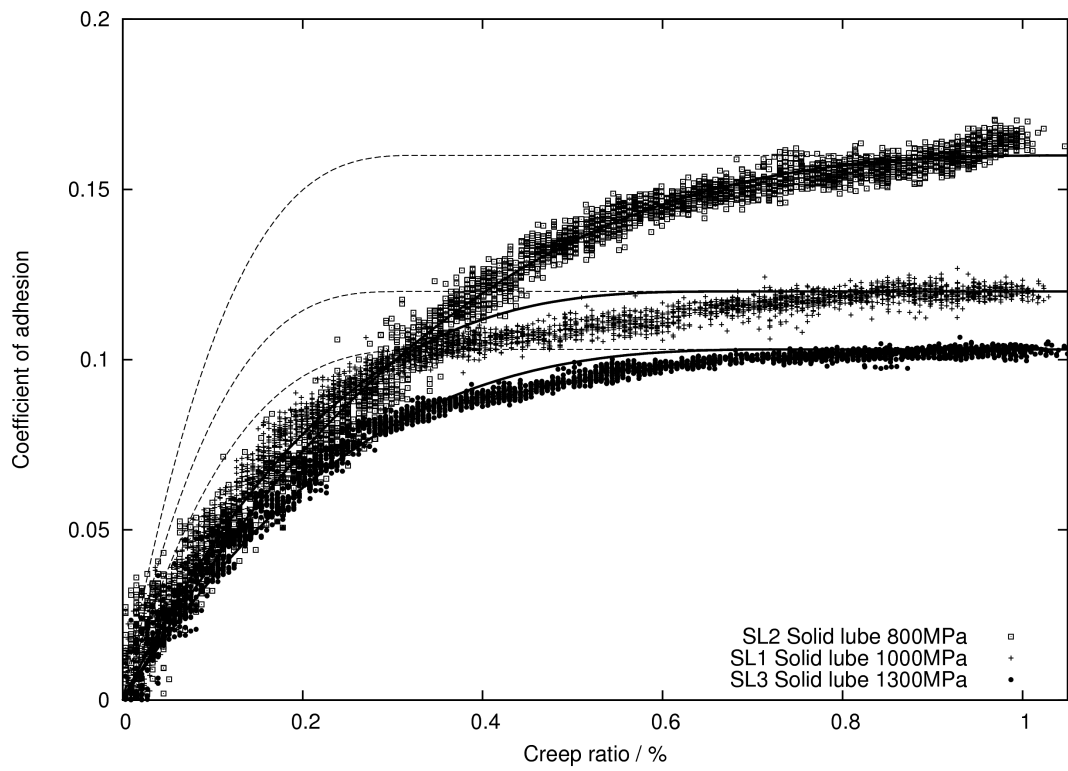


Figure 5

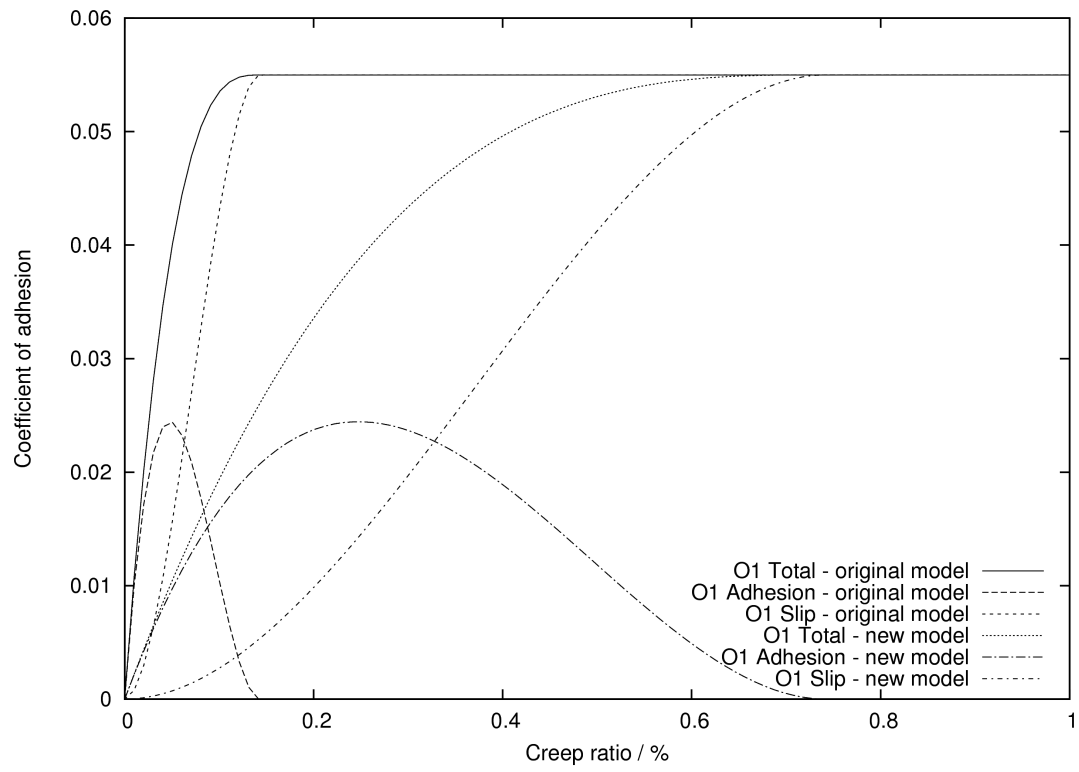


Figure 6.